

## INTEGRAL FIELD SPECTROSCOPY OF MASSIVE, KILOPARSEC-SCALE OUTFLOWS IN THE INFRARED-LUMINOUS QSO MRK 231

DAVID S. N. RUPKE

Department of Physics, Rhodes College, Memphis, TN 38112

AND SYLVAIN VEILLEUX

Department of Astronomy, University of Maryland, College Park, MD 20742

Received 2010 December 17; accepted 2011 February 1; published 2011 March 10

### ABSTRACT

The quasi-stellar object (QSO)/merger Mrk 231 is arguably the nearest and best laboratory for studying QSO feedback. It hosts several outflows, including broad-line winds, radio jets, and a poorly-understood kpc scale outflow. In this Letter, we present integral field spectroscopy from the Gemini telescope that represents the first unambiguous detection of a wide-angle, kpc scale outflow from a powerful QSO. Using neutral gas absorption, we show that the nuclear region hosts an outflow with blueshifted velocities reaching  $1100 \text{ km s}^{-1}$ , extending  $2 - 3 \text{ kpc}$  from the nucleus in all directions in the plane of the sky. A radio jet impacts the outflow north of the nucleus, accelerating it to even higher velocities (up to  $1400 \text{ km s}^{-1}$ ). Finally,  $3.5 \text{ kpc}$  south of the nucleus, star formation is simultaneously powering an outflow that reaches more modest velocities of only  $570 \text{ km s}^{-1}$ . Blueshifted ionized gas is also detected around the nucleus at lower velocities and smaller scales. The mass and energy flux from the outflow are  $\gtrsim 2.5$  times the star formation rate and  $\gtrsim 0.7\%$  of the active galactic nucleus luminosity, consistent with negative feedback models of QSOs.

*Subject headings:* galaxies: evolution — galaxies: ISM — galaxies: jets — galaxies: kinematics and dynamics — quasars: individual (Mrk 231)

### 1. INTRODUCTION

Theory predicts that negative feedback in active galactic nuclei (AGNs) regulates the growth of supermassive black holes and their accompanying starbursts (Di Matteo et al. 2005; Narayanan et al. 2008; Hopkins & Elvis 2010). On the scales of galaxies, radio jets power neutral and ionized outflows with significant mass and energy flux (Morganti et al. 2005, 2007; Holt et al. 2008; Fu & Stockton 2009; Holt et al. 2011). Wide-angle outflows on sub-kiloparsec scales are also common in radio-quiet systems (e.g., Crenshaw & Kraemer 2005). Precisely how and to what degree these phenomena are the negative feedback predicted by theory is an area of active study.

The ultraluminous infrared galaxy (ULIRG) Mrk 231, the nearest infrared-luminous quasi-stellar object (QSO), is a unique system because it hosts several types of AGN outflows. It also combines many of the phenomena of interest in models of galaxy mergers that then form powerful QSOs (e.g., Sanders et al. 1988; Hopkins et al. 2005). The nuclei in Mrk 231 have coalesced, but prominent features of an interaction are still present (e.g., Surace et al. 1998). It contains a powerful, unobscured AGN alongside an obscured starburst (Veilleux et al. 2009). Finally, several types of outflows are present: pc and kpc-scale radio jets (Carilli et al. 1998; Ulvestad et al. 1999); a low ionization, broad absorption line outflow with blueshifted velocities up to  $8000 \text{ km s}^{-1}$  (e.g., Boksenberg et al. 1977; Boroson et al. 1991), presumably arising at pc scales; and a kpc scale outflow with velocities exceeding  $1000 \text{ km s}^{-1}$ .

The properties of this third outflow concern us here.

Blueshifted emission lines led to speculation of its existence (Hamilton & Keel 1987; Krabbe et al. 1997), but emission lines are subject to misinterpretation, as blueshifted lines could indicate inflow or outflow (e.g., Veilleux 1991). Using long slit observations, Rupke et al. (2005a) showed conclusive evidence that a  $\gtrsim 1000 \text{ km s}^{-1}$  neutral outflow was present at galactocentric radii up to  $3 \text{ kpc}$ . More recently, this outflow was detected in the molecular phase at very similar velocities, with a marginal detection of extended emission (Fischer et al. 2010; Feruglio et al. 2010).

The structure and power source of this outflow have remained elusive. Though the high velocities suggested the influence of the AGN was helping to power the wind, Rupke et al. (2005a) were unable to determine whether the wind was powered by the jet or more widely-directed AGN energy, and what role the starburst played. The high molecular gas velocities observed (Fischer et al. 2010; Feruglio et al. 2010) also suggest AGN influence, but the spatial resolution of these observations made the power source equally difficult to determine.

In this Letter, we present integral field spectroscopy of the outflow in Mrk 231, probing both the neutral and ionized phases using Na I D  $5890, 5896 \text{ \AA}$  interstellar absorption and the  $\text{H}\alpha / [\text{N II}]$  emission-line complex. Using sub-kpc spatial resolution, we untangle the structure and dynamics of the outflow and show that jets, wide-angle AGN influence, and the starburst all play a role in moving large amounts of gas out of the central regions of this galaxy.

### 2. OBSERVATIONS, REDUCTION, AND ANALYSIS

Mrk 231 was observed on 2007 July 7 UT with the Integral Field Unit in the Gemini Multi-Object Spectrograph (GMOS; Allington-Smith et al. 2002; Hook et al. 2004) on the Gemini North telescope. Cloud cover was minimal, and image quality was very high ( $0''.5 - 0''.6$ ). We obtained five exposures of 900 s each, at a position angle of  $35^\circ$  to ensure that diffraction spikes from the nuclear point source were not oriented along the north-south jet axis. Our dither pattern centered on the nucleus, with exposures alternating  $\pm 1''.5$  along one of the field axes. We used the integral field unit in two-slit mode and the B600 grating, yielding wavelength coverage from 5600 to 6950 Å and a spectral resolution of  $1.80\text{Å}$  at  $6300\text{Å}$ .

We reduced the data using the IRAF data reduction package provided by the Gemini Observatory, supplemented with custom IDL routines. The  $0''.3$  spaxels in the final data cube maximize signal-to-noise ratio while adequately sampling the seeing disk. The resulting cube contains 525 spectra and measures  $6''.3 \times 7''.5$ , with the long axis oriented northeast to southwest.

We modeled the continuum and emission lines in each spectrum using UHSPECFIT, a suite of IDL routines that fits a continuum and emission lines to spectra (Rupke et al. 2010). We fit the continuum at each point as a linear combination of the nuclear spectrum and a smooth host galaxy continuum. Where possible, we fit two Gaussian velocity components to the emission lines. One component represents the narrow, rotating velocity component, and the second represents an underlying broad, blueshifted component.

We modeled the Na I D absorption lines using the method of Rupke et al. (2005b). One velocity component provided good fits throughout the cube. The nearby He I 5876 Å emission line was parameterized using the fit to other lines, but in almost all spaxels this line was absent or very weak.

Figure 1 shows six example fits to the emission and absorption lines. They illustrate the high quality of the fits.

Our line profile modeling is based on Gaussian velocity profiles. As such, we define outflow velocities in this Letter based on the properties of the normal distribution. We define negative velocities to be blueshifted and outflowing.

$$\begin{aligned} v_{50\%} &\equiv \text{center of Gaussian profile} \\ & \text{(50\% of gas has lower outflow velocity)} \quad (1) \end{aligned}$$

$$\begin{aligned} v_{84\%} &\equiv v_{50\%} - \sigma \\ & \text{(84\% of gas has lower outflow velocity)} \quad (2) \end{aligned}$$

$$\begin{aligned} v_{98\%} &\equiv v_{50\%} - 2\sigma \\ & \text{(98\% of gas has lower outflow velocity)} \quad (3) \end{aligned}$$

### 3. RESULTS

#### 3.1. Host Galaxy

Our data reproduce known properties of the host galaxy in Mrk 231. Figure 2 shows the entire galaxy, with the GMOS field of view superimposed.  $H\alpha$  emission traces young star formation, including the edge of a prominent blue arc  $\sim 5$  kpc south of the nucleus (Surace et al. 1998). The  $[\text{N II}]/H\alpha$  map reveals high excitation outside of star forming regions; high extranuclear excitation is common in ULIRGs (Veilleux et al. 1995;

Monreal-Ibero et al. 2006).

The rotation of the central gas disk of Mrk 231 has been modeled using CO observations (Bryant & Scoville 1996; Downes & Solomon 1998), yielding a projected velocity amplitude of  $70 \text{ km s}^{-1}$  along the  $90^\circ$  line of nodes and a disk inclination of  $10^\circ - 20^\circ$ . This molecular gas is concentrated in a  $r \sim 1$  kpc disk (Downes & Solomon 1998). From CO and H I observations (Downes & Solomon 1998; Carilli et al. 1998), we adopt a systemic velocity of  $z = 0.0422$ . This yields a spatial scale of  $0.867 \text{ kpc arcsec}^{-1}$ .

The rotation of the ionized gas lines up with that of the molecular component, despite the difference in extinction of the two components (Figure 3). Our data trace this rotation to larger radii than the CO observations. Deviations from the typical galaxy rotation curve are evident, but discussion of these features is outside the scope of this Letter.

#### 3.2. Outflow

The second ionized gas component is blueshifted and much broader than the rotating component. Within 1.5 kpc of the nucleus, the center velocity of the second component averages  $\langle v_{50\%} \rangle = -150 \text{ km s}^{-1}$ , with larger velocities closer to the nucleus. Because these components are also very broad, with  $\langle \text{FWHM} \rangle = 700 \text{ km s}^{-1}$ , the ionized gas reaches  $\langle v_{98\%} \rangle = -760 \text{ km s}^{-1}$ . The region of broad, blueshifted emission is asymmetric, with higher velocities to the north and more extended emission to the east.

The neutral atomic gas in Mrk 231, as traced by Na I D, is strikingly different from the ionized gas (Figure 4). At the  $4\sigma$  level, Na I D absorption extends from radii of 0.5 to 3 kpc, which is farther than the ionized outflow. (Closer than 0.5 kpc, the nuclear emission washes out the signature of the host galaxy.) A significant area of absorption is also seen atop the blue continuum peak 3.5 kpc south of the nucleus.

The neutral gas velocities are also much higher than the ionized gas velocities. The Na I D velocity maps consist of three distinct regions, whose velocity averages are found in Table 1. The lowest velocities lie atop the southern star-forming arc. Higher velocity, broader components are found in the outflow surrounding the nucleus (not including the northern quadrant). The highest velocities are found in the northern quadrant of the nuclear outflow. In those parts of the northern quadrant that line up with the radio jet in Mrk 231, the velocities reach  $-1400 \text{ km s}^{-1}$ .

The velocities observed in the arc are comparable to those measured in starburst-dominated ULIRGs (Table 1; Martin 2005; Rupke et al. 2005c). However, those in the nuclear wind are significantly higher; they are more like those found in some Seyfert ULIRGs (Rupke et al. 2005a; Krug et al. 2010).

### 4. DISCUSSION

ULIRGs host powerful starburst-driven outflows (Heckman et al. 1990, 2000) that arise in all ULIRGs (Rupke et al. 2005c) and show kpc scale extents (Martin 2006; Shih & Rupke 2010). They have  $\langle v_{98\%} \rangle = -450 \text{ km s}^{-1}$  in systems whose infrared luminosity is dominated by star formation (Rupke et al. 2005c; Martin

2005). Rupke et al. (2005c) calculate that ULIRG mass outflow rates are 20% of the star formation rate on average. However, evidence has remained elusive for large-scale outflows that are clearly AGN-driven in LIRGs or ULIRGs (Rupke et al. 2005a).

The data we present here are clear: there is a neutral,  $\sim 1000 \text{ km s}^{-1}$  outflow in Mrk 231 that extends in every direction from the nucleus (as projected into the plane of the sky) out to at least 3 kpc. Such high velocities have not been seen in starburst ULIRGs (Table 1), providing strong circumstantial evidence that this wide-angle nuclear wind is driven by radiation or mechanical energy from the AGN.

From what we know about the structure of galactic winds (Veilleux et al. 2005), the molecular disk in Mrk 231 collimates this nuclear wind. Given the disk’s almost face-on orientation, we must be looking “down the barrel” of a biconical outflow. The other end of this bicone is receding from us, behind the galaxy disk and therefore invisible at optical wavelengths.

It is apparent from the velocity map that the north–south radio jet in Mrk 231 (Carilli et al. 1998; Ulvestad et al. 1999) is coupling to the nuclear wind, accelerating the neutral gas to even higher velocities. The jet is not constrained to emerge perpendicular to the disk, and thus produces an asymmetric effect. The present data imply that the northern arm of the large-scale jet is on the near side of the molecular disk. Neutral outflows driven by jet interactions with the interstellar medium (ISM) on kpc scales have also been observed in radio galaxies in H I absorption (Morganti et al. 2005, 2007). The newly discovered jet-wind interaction in Mrk 231 appears to be similar, though this time the jet accelerates an already in situ wind.

Carilli et al. (1998) and Taylor et al. (1999) studied the diffuse radio continuum emission from Mrk 231, which is symmetric about the nucleus on scales of 100 pc to 1 kpc. They hypothesized that this emission is produced by in situ electron acceleration, but could not rule out that the AGN distributes these electrons through a wide-angle outflow. Our data are further evidence for the in situ interpretation, since we now know that the AGN outflow reaches larger scales and is asymmetrically accelerated.

Along with these AGN-driven outflows, Mrk 231 also hosts a starburst-driven wind. Blueshifted velocities with  $\langle v_{98\%} \rangle = -570 \text{ km s}^{-1}$  are observed in the star-forming arc south of the nucleus. These are comparable to the maximum velocities observed in other starburst ULIRGs (Table 1). We cannot rule out that the underlying continuum could be backlighting the nuclear wind at this location. However, a simpler explanation is that in situ star formation is driving an off-nuclear wind.

The ionized outflow in Mrk 231 overlaps spatially with the neutral outflow near the nucleus and shows broad velocity profiles. It also shows higher velocities to the north. However, the velocities and extent of this wind phase are more modest. The ionized outflow in Mrk 231 could be another phase of the nuclear wind, providing further evidence that the different gas phases in ULIRG winds are not strongly coupled (Rupke et al. 2005a; Shih & Rupke 2010). It may also be the classic AGN narrow line region (e.g., Crenshaw & Kraemer 2005).

The nuclear wind is clearly the one detected previously in the neutral (Rupke et al. 2005c) and molecular (Fis-

cher et al. 2010; Feruglio et al. 2010) phases. Rupke et al. (2005c) found an extended wind (on kpc scales), but only had data in a north-south slice. Feruglio et al. (2010) marginally resolved the molecular component out to radii of  $\sim 0.6 \text{ kpc}$ , and estimated molecular mass and energy fluxes of several hundred  $M_{\odot} \text{ yr}^{-1}$  and  $\sim 10^{44} \text{ erg s}^{-1}$ .

The current data are a significant improvement on these results. They clearly resolve the structure of the wind on sub-kpc scales and reveal that more than one power source is acting. To produce a wide-angle outflow, the AGN energy and momentum must be injected into the ISM over a substantial volume through mechanical or radiative processes. Either (1) wide-angle winds from the AGN accretion disk or broad line region or (2) coupling of the AGN radiation to the dust in the wind are possible explanations (e.g., Crenshaw et al. 2003; Hopkins & Elvis 2010). However, the high-velocity component of the wind that lies north of the nucleus must experience an additional, asymmetric force. The north-south jet in Mrk 231 is a natural explanation.

Using a simple model, we can estimate the mass and energy fluxes ( $\dot{M}$  and  $\dot{E}$ ) in the nuclear wind (Rupke et al. 2005c; Shih & Rupke 2010). We assume a face-on wind for simplicity. We model the wind as emanating from the nucleus in a thin shell, and compute a time-averaged mass flux. Rupke et al. (2005c) also discuss a thick-shell model. However, computing the mass outflow rate for this model would require integrating hypothetical velocity profiles over each line of sight; such an exercise is beyond the scope of this Letter and would increase the number of unconstrained parameters.

There are two significant unknowns in the thin shell model. The first is the radius of the shell. Given the spatial smoothness of the Na I D velocity map, it must be larger than 2 kpc, or we would observe the velocity to decrease (in projection) with increasing radius. However, it cannot be too large, or we would observe a more extended absorption region. We use a fiducial radius of 3 kpc; larger values will increase the resulting  $\dot{M}$  and  $\dot{E}$ . The second uncertainty is the ionization state of Na. As in previous work (e.g., Rupke et al. 2005b), we use Milky Way measurements as a baseline and assume  $N(\text{Na I})/N(\text{Na}) = 1 - y = 0.1$ , where  $y$  is the ionization fraction. The fluxes are inversely proportional to  $(1 - y)$ , such that a more ionized wind will yield higher  $\dot{M}$  and  $\dot{E}$ .

With this model, we compute  $\dot{M} = 420 (R/3 \text{ kpc}) [0.1/(1 - y)] M_{\odot} \text{ yr}^{-1}$  and  $\dot{E} = 7.3 \times 10^{43} (R/3 \text{ kpc}) [0.1/(1 - y)] \text{ erg s}^{-1}$ . For comparison, the star formation rate and AGN luminosity in Mrk 231 are  $172 M_{\odot} \text{ yr}^{-1}$  and  $1.1 \times 10^{46} \text{ erg s}^{-1}$ . (These numbers are computed by assuming the bulk of the galaxy’s radiation emerges in the far-infrared, using the AGN contribution to Mrk 231’s bolometric luminosity from Veilleux et al. 2009, and calculating the star formation rate with the formula from Kennicutt 1998.) The wind is clearly removing significant amounts of gas from the nucleus – at a level of 2.5 times the star formation rate. This mass outflow rate is also strikingly similar to that estimated by Feruglio et al. (2010) from a different tracer.

The energy outflow rate is about 0.7% of the radiative luminosity of the AGN, meaning that only a small

part of the radiative output of the AGN has to couple to the outflow. This is remarkably similar to the required coupling efficiency needed for an AGN wind in the two-phase model of Hopkins & Elvis (2010). In this model, the AGN couples to the hot ISM, driving a diffuse outflow. This diffuse outflow disrupts cold clouds, which are propelled outward by the diffuse wind and by radiation pressure from the AGN. Together, the hot and cold winds provide negative feedback on the AGN and star formation.

## 5. SUMMARY

The galaxy Mrk 231 is in the late stages of a major merger, hosts a QSO and an obscured starburst, and exhibits gas outflows in multiple forms. We show in this Letter that there is a massive, energetic, and neutral outflow extending in all directions from the nucleus (as projected in the plane of the sky) to radii of at least 3 kpc. This outflow has blueshifted velocities that reach  $1100 \text{ km s}^{-1}$ . On the axis of the radio jet in Mrk 231,  $v_{98\%}$  is as large as  $1400 \text{ km s}^{-1}$ . Mass and energy outflow rates are  $\gtrsim 2.5 \times$  the star formation rate and  $\gtrsim 0.7\%$  of the AGN luminosity. The former suggests strong negative feedback to star formation, and the latter is consistent with the coupling efficiency required in the AGN feedback model of Hopkins & Elvis (2010).

By comparing the velocities in this wind to those in the average starburst-driven ULIRG, we conclude that this wide-angle wind is likely powered by the central AGN, and its power source must be directed fairly symmetrically. The northern quadrant of this nuclear outflow experiences additional acceleration due to the radio jet in Mrk 231. Furthermore, a starburst-powered wind arises in the extended galaxy disk to the south of the nucleus.

These data illuminate the structure and power source of the kpc scale wind in Mrk 231, and show that strong feedback occurs as a result. The ubiquity of winds in major mergers is well-known, but our understanding of their full impact on galaxy evolution is improving through integral field observations (Shih & Rupke 2010 and the present work), Herschel studies (Fischer et al. 2010; Sturm et al. 2010), and ground-based molecular observations (Feruglio et al. 2010).

This Letter was based on observations obtained at the Gemini Observatory, which is operated by AURA under a cooperative agreement with NSF on behalf of the Gemini partnership. It also made use of NASA/ESA *Hubble Space Telescope* data obtained from the Hubble Legacy Archive. S.V. acknowledges partial support by the National Science Foundation through AST/EXC grants AST0606932 and AST1009583.

## REFERENCES

- Allington-Smith, J. et al. 2002, PASP, 114, 892, ADS  
 Boksenberg, A., Carswell, R. F., Allen, D. A., Fosbury, R. A. E., Penston, M. V., & Sargent, W. L. W. 1977, MNRAS, 178, 451, ADS  
 Boroson, T. A., Meyers, K. A., Morris, S. L., & Persson, S. E. 1991, ApJ, 370, L19, ADS  
 Bryant, P. M., & Scoville, N. Z. 1996, ApJ, 457, 678, ADS  
 Carilli, C. L., Wrobel, J. M., & Ulvestad, J. S. 1998, AJ, 115, 928, ADS  
 Crenshaw, D. M., & Kraemer, S. B. 2005, ApJ, 625, 680, arXiv:astro-ph/0501257  
 Crenshaw, D. M., Kraemer, S. B., & George, I. M. 2003, ARA&A, 41, 117, ADS  
 Di Matteo, T., Springel, V., & Hernquist, L. 2005, Nature, 433, 604, arXiv:astro-ph/0502199  
 Downes, D., & Solomon, P. M. 1998, ApJ, 507, 615, arXiv:astro-ph/9806377  
 Feruglio, C., Maiolino, R., Piconcelli, E., Menci, N., Aussel, H., Lamastra, A., & Fiore, F. 2010, A&A, 518, L155, 1006.1655  
 Fischer, J. et al. 2010, A&A, 518, L41, 1005.2213  
 Fu, H., & Stockton, A. 2009, ApJ, 690, 953, 0809.1117  
 Hamilton, D., & Keel, W. C. 1987, ApJ, 321, 211, ADS  
 Heckman, T. M., Armus, L., & Miley, G. K. 1990, ApJS, 74, 833, ADS  
 Heckman, T. M., Lehnert, M. D., Strickland, D. K., & Armus, L. 2000, ApJS, 129, 493, arXiv:astro-ph/0002526  
 Holt, J., Tadhunter, C. N., & Morganti, R. 2008, MNRAS, 387, 639, 0802.1444  
 Holt, J., Tadhunter, C. N., Morganti, R., & Emonts, B. H. C. 2011, MNRAS, 410, 1527, 1008.2846  
 Hook, I. M., Jørgensen, I., Allington-Smith, J. R., Davies, R. L., Metcalfe, N., Murowinski, R. G., & Crampton, D. 2004, PASP, 116, 425, ADS  
 Hopkins, P. F., & Elvis, M. 2010, MNRAS, 401, 7, 0904.0649  
 Hopkins, P. F., Hernquist, L., Cox, T. J., Di Matteo, T., Martini, P., Robertson, B., & Springel, V. 2005, ApJ, 630, 705, arXiv:astro-ph/0504190  
 Kennicutt, R. C., J. 1998, ARA&A, 36, 189, arXiv:astro-ph/9807187  
 Krabbe, A., Colina, L., Thatte, N., & Kroker, H. 1997, ApJ, 476, 98, ADS  
 Krug, H. B., Rupke, D. S. N., & Veilleux, S. 2010, ApJ, 708, 1145, 0911.3897  
 Martin, C. L. 2005, ApJ, 621, 227, arXiv:astro-ph/0410247  
 —. 2006, ApJ, 647, 222, arXiv:astro-ph/0604173  
 Monreal-Ibero, A., Arribas, S., & Colina, L. 2006, ApJ, 637, 138, arXiv:astro-ph/0509681  
 Morganti, R., Holt, J., Saripalli, L., Oosterloo, T. A., & Tadhunter, C. N. 2007, A&A, 476, 735, 0710.1189  
 Morganti, R., Oosterloo, T. A., Tadhunter, C. N., van Moorsel, G., & Emonts, B. 2005, A&A, 439, 521, arXiv:astro-ph/0505365  
 Narayanan, D. et al. 2008, ApJS, 176, 331, 0710.0384  
 Rupke, D. S., Veilleux, S., & Sanders, D. B. 2005a, ApJ, 632, 751, arXiv:astro-ph/0507037  
 —. 2005b, ApJS, 160, 87, arXiv:astro-ph/0506610  
 —. 2005c, ApJS, 160, 115, arXiv:astro-ph/0506611  
 Rupke, D. S. N., Kewley, L. J., & Chien, L. 2010, ApJ, 723, 1255, 1009.0761  
 Sanders, D. B., Soifer, B. T., Elias, J. H., Madore, B. F., Matthews, K., Neugebauer, G., & Scoville, N. Z. 1988, ApJ, 325, 74, ADS  
 Shih, H., & Rupke, D. S. N. 2010, ApJ, 724, 1430, 1009.6020  
 Sturm, E. et al. 2010, ApJ, submitted  
 Surace, J. A., Sanders, D. B., Vacca, W. D., Veilleux, S., & Mazzarella, J. M. 1998, ApJ, 492, 116, ADS  
 Taylor, G. B., Silver, C. S., Ulvestad, J. S., & Carilli, C. L. 1999, ApJ, 519, 185, arXiv:astro-ph/9902082  
 Ulvestad, J. S., Wrobel, J. M., & Carilli, C. L. 1999, ApJ, 516, 127, arXiv:astro-ph/9901190  
 Veilleux, S. 1991, ApJ, 369, 331, ADS  
 Veilleux, S., Cecil, G., & Bland-Hawthorn, J. 2005, ARA&A, 43, 769, arXiv:astro-ph/0504435  
 Veilleux, S., Kim, D.-C., Sanders, D. B., Mazzarella, J. M., & Soifer, B. T. 1995, ApJS, 98, 171, ADS  
 Veilleux, S. et al. 2009, ApJS, 182, 628, 0905.1577

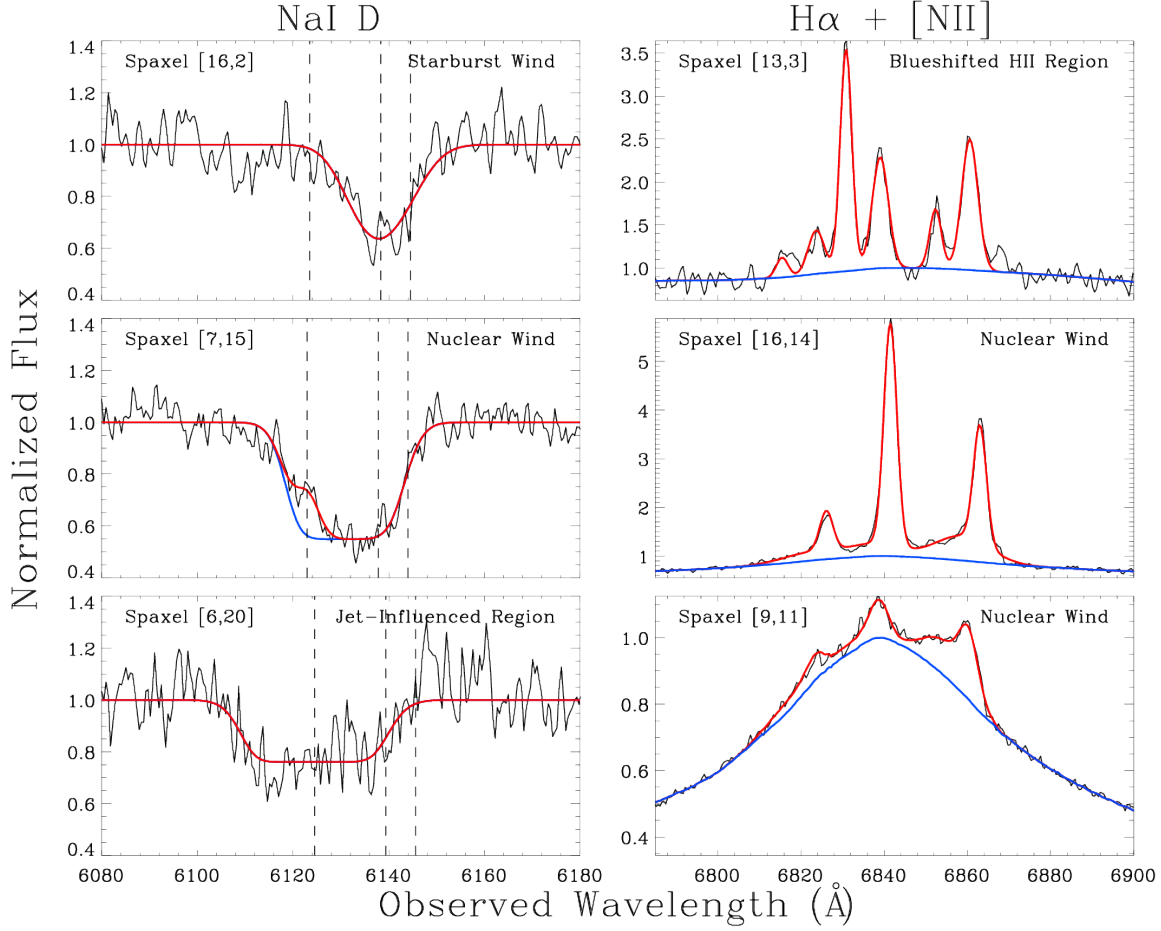


**Figure 1.** Left: absorption line fits to Na I D. One spectrum is shown in each major outflow region (Sections 3.2 and 4). The spaxel coordinates of each fit are shown in the upper left of each plot; the nucleus is located at spaxel [11,13], and spaxels are  $0''.3$  in size. The vertical dashed lines show the locations of He I 5876 Å and Na I D according to the rotation curve. The red line is the total (absorption + emission) fit, while the blue line is absorption only. Right: emission line fits to the H $\alpha$  / [N II] spectral region. The red line is the total (extended line emission + broad line region emission + continuum) fit, while the blue line is broad line region emission + continuum only.

**Table 1**  
Outflow Velocities in Mrk 231

Label (1)	Phase (2)	$\langle \text{FWHM} \rangle$ (3)	$\langle v_{50\%} \rangle$ (4)	$\langle v_{84\%} \rangle$ (5)	$\langle v_{98\%} \rangle$ (6)
Mrk 231 starburst wind	Neutral	510	-150	-360	-570
Mrk 231 nuclear wind	Neutral	600	-360	-620	-880
...	Ionized <sup>a</sup>	690	-160	-450	-750
Mrk 231 jet-influenced region	Neutral	640	-520	-800	-1070
Starburst ULIRGs <sup>b</sup>	Neutral	330	-170	-310	-450

**Note.** — Column 2: gas phase. Column 3: full width at half maximum of velocity distribution, in  $\text{km s}^{-1}$ . Column 4: velocity at the center of (Gaussian) velocity distribution. Column 5:  $v_{84\%} \equiv v_{50\%} - \sigma$ ; 84% of the outflowing gas has velocities closer to 0. Column 6:  $v_{98\%} \equiv v_{50\%} - 2\sigma$ .

<sup>a</sup> For the broad, outflowing component.

<sup>b</sup> Computed from starburst-driven ULIRGs in Rupke et al. (2005c). This is a sample average, as opposed to the spatial average for Mrk 231.

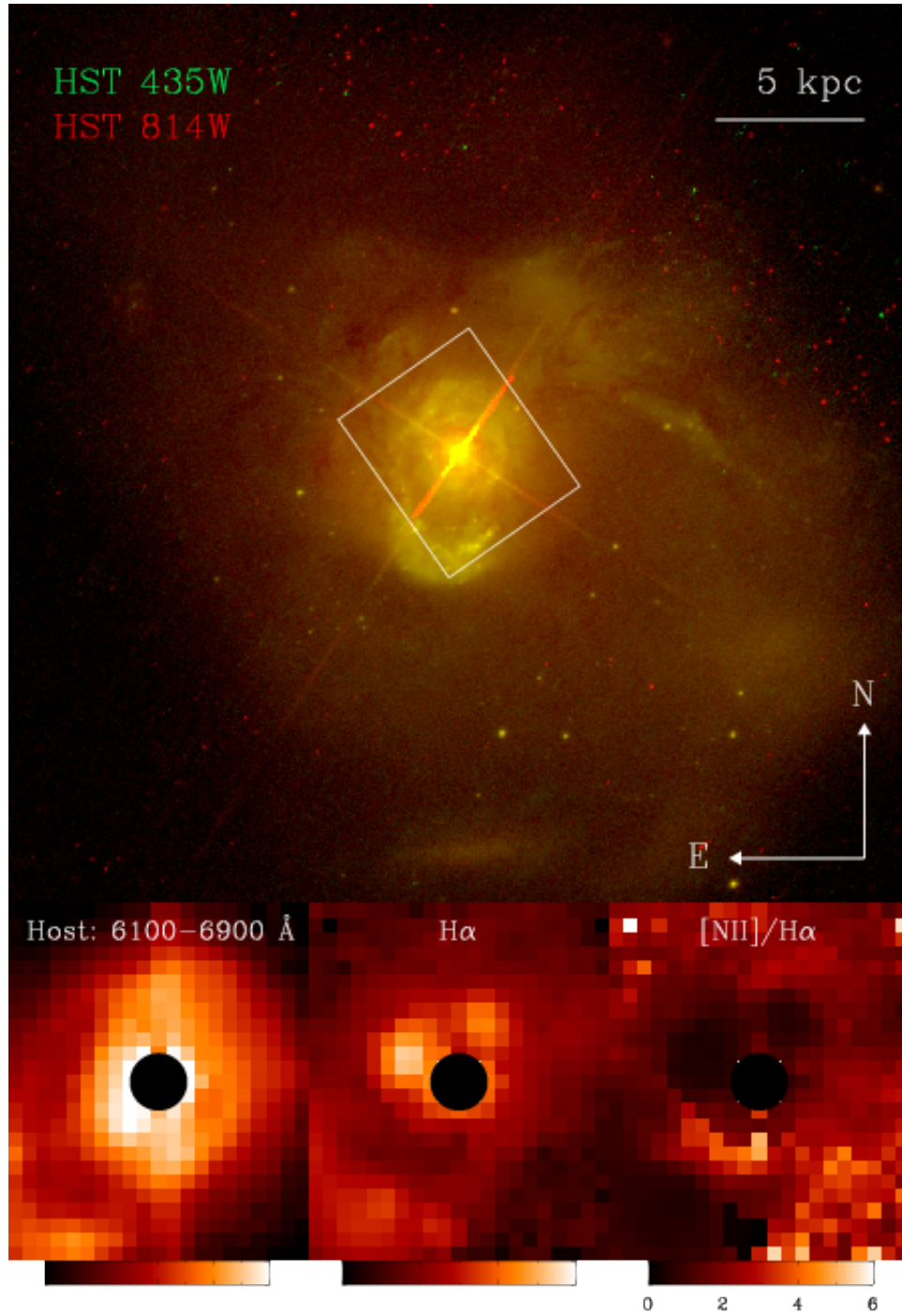


**Figure 2.** Top: continuum image of Mrk 231 in the 435W and 814W filters, from *Hubble Space Telescope* observations with the Advanced Camera for Surveys. The field of view of our GMOS data ( $6''.3 \times 7''.5$ ) is overlaid as a box. Bottom left: host galaxy continuum image in our GMOS field, summed over the wavelength range 6100 – 6900 Å, in logarithmic flux units. Bottom center: H $\alpha$  emission, in logarithmic flux units. Bottom right: map of the [N II] $\lambda$ 6583/H $\alpha$  flux ratio.

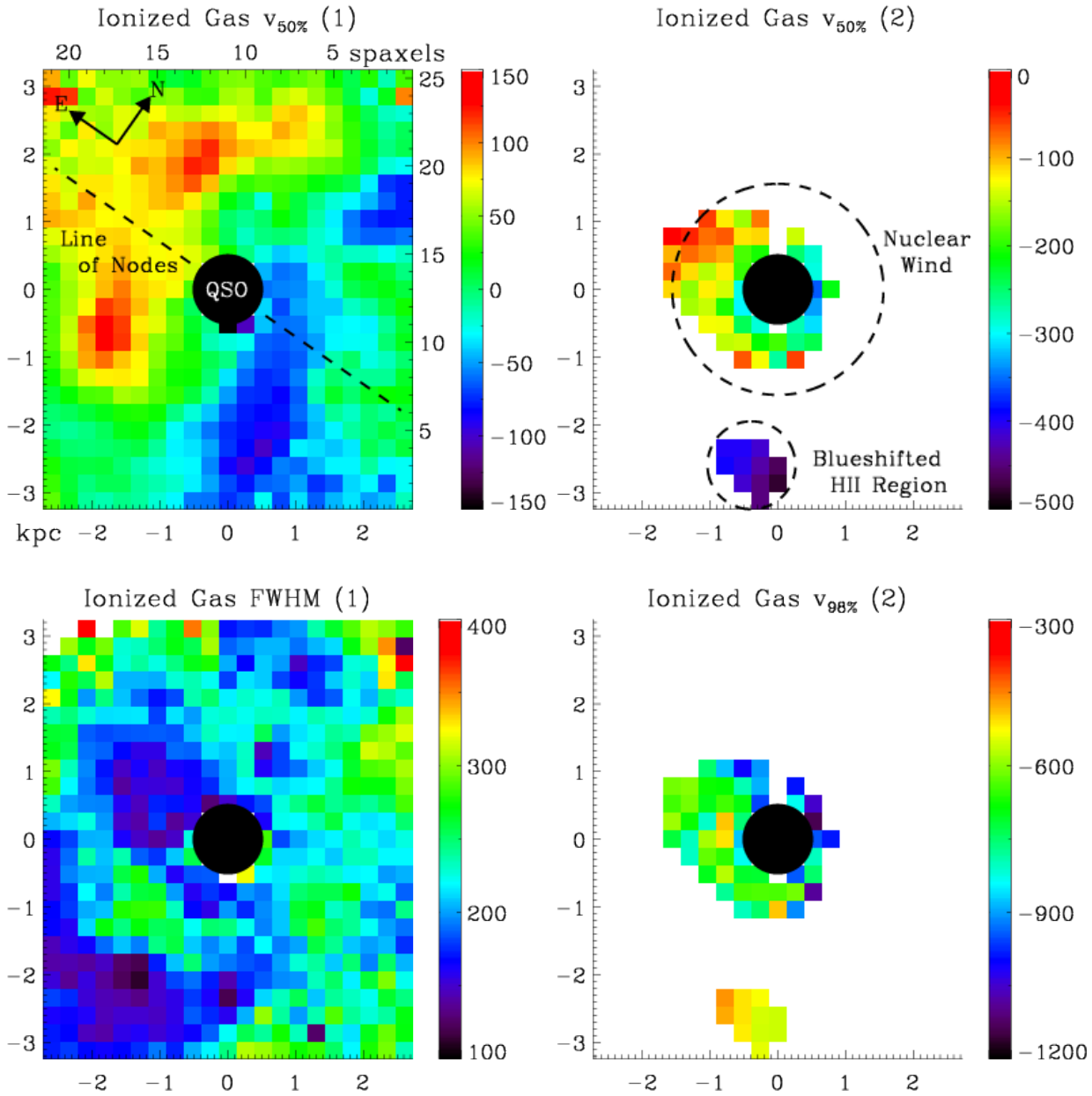


**Figure 3.** Left: central velocity and FWHM maps of the rotating ionized gas component, in  $\text{km s}^{-1}$ . The ionized gas rotation is consistent with that of the nuclear molecular disk. The line of nodes position angle is from Downes & Solomon (1998). Right:  $v_{50\%}$  and  $v_{98\%}$  (Section 2) for the broad, outflowing ionized gas component. A near-nuclear outflow is present, as well as a highly blueshifted H II region in the southwest.

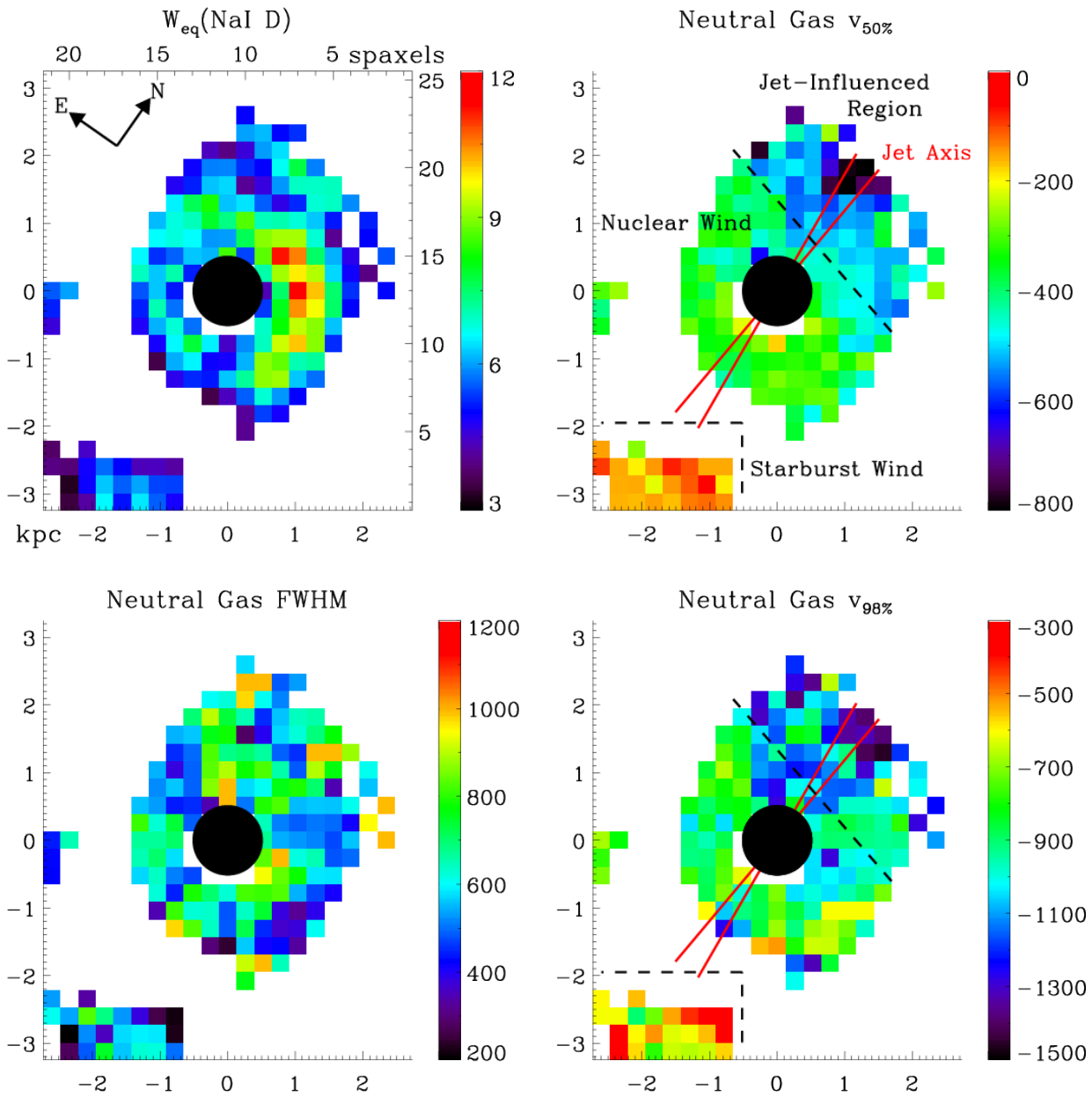


**Figure 4.** Equivalent width, central velocity, FWHM, and  $v_{98\%}$  maps of Na I D. A nuclear outflow extends from the nucleus up to 2–3 kpc in all directions (as projected in the plane of the sky). The high velocities suggest that the AGN powers the nuclear wind. The northern quadrant of the nuclear wind is further accelerated by the radio jet. A lower-velocity starburst-driven outflow is present in the south.